

Signal Analysis of Urban Channels in Broadband Wireless Communication Based on
Radio Wave Propagation Simulation by Parallel FDTD Algorithm.

Glen Rodriguez*, Yasumitsu Miyazaki**, and Nobuo Goto*

* Toyohashi University of Technology ** Aichi University of Technology

* Hibarigaoka 1-1, Tempaku-cho Toyohashi-shi, 441-8580, JAPAN

** Umanori 50-2, Nishihasama-cho, Gamagori-shi, 443-0047, JAPAN

miyazaki@aut.ac.jp

1. Introduction

This paper presents the studies on wave propagation for systems and channels of broadband, high-speed wireless communication using a new parallel FDTD method applied to large 2-D areas. Analysis of multipath propagation in urban areas for high-speed wireless communication is very important in order to improve the system. High accuracy is necessary, and the best kind of numerical method is a full solution of Maxwell equations as the FDTD method. We have created a parallel FDTD algorithm for dealing with big urban area models. Using this method, we have created a microcell urban model based on FDTD results and we have evaluated TDMA and CDMA modulation.

2. Mathematical basis of the method

For linear materials, the 2-D TM FDTD formulation can be represented as a set of linear equations, with variables E_z , H_x and H_y , as in eq.(1)-(3), where C_a , C_x , C_y , D_x and D_y are constants respect the m-th material. X_i is a vector containing all the variables for time step i, the relation between variables in time step i and i+1 is $X_{i+1} = A_i X_i + \phi_i$, where ϕ_i represents source of currents and A_i is a constant matrix. We can represent all the FDTD simulation as the a system of linear equations, as seen in [1],[2], as shown in eq.(4):

$$E_z^{n+1}(i, j) = C_a(m)E_z^n(i, j) + C_x(m)[H_y^n(i+1, j) - H_y^n(i, j)] - C_y(m)[H_x^n(i, j+1) - H_x^n(i, j)] \quad (1)$$

$$H_x^{n+1}(i, j) = H_x^{n+1}(i, j) - D_y(m)[E_z^{n+1}(i, j) - E_z^{n+1}(i, j-1)] \quad (2)$$

$$H_y^{n+1}(i, j) = H_y^{n+1}(i, j) - D_x(m)[E_z^{n+1}(i, j) - E_z^{n+1}(i-1, j)] \quad (3)$$

$$\begin{bmatrix} I & 0 & \cdots & 0 & 0 \\ -A_1 & I & \cdots & 0 & 0 \\ \vdots & \vdots & \ddots & \vdots & \vdots \\ 0 & 0 & \cdots & I & 0 \\ 0 & 0 & \cdots & -A_1 & I \end{bmatrix} \begin{bmatrix} X_1 \\ X_2 \\ \vdots \\ X_{T-1} \\ X_T \end{bmatrix} = \begin{bmatrix} \phi_1 \\ \phi_2 \\ \vdots \\ \phi_{T-1} \\ \phi_T \end{bmatrix} \quad (4)$$

The solution of FDTD becomes equivalent to solution of this system by Gaussian substitution. Substitution would require a lot of memory, but we carry out the solution in partial stages, solving eq.(5), where x_L is a wanted variable (E_z , H_x or H_y) at some time step t and position (i,j), depending on other variables x_k^{t-1} of time step t-1. Substitution is done until eq.(5) becomes eq.(6). Where the variables x_k^n are components of the fields in time step t-n. We repeat this process for solving each variable x_k^n as a new x_L . The equations are stored in different arrays on many processors, computing in parallel subsets of x_k^n . Memory can be saved because not all the variables are required to be in memory simultaneously.

$$x_L + c_1^1 x_1^1 + c_2^1 x_2^1 + \dots + c_{z_1}^1 x_{z_1}^1 = b_L^1 \quad (5)$$

$$x_L + c_1^n x_1^n + c_2^n x_2^n + \dots + c_{z_n}^n x_{z_n}^n = b_L^1 \quad (6)$$

In order to improve the speed of the algorithm, numerical Green's function were used. In a linear system, we have that the values of Green's function $g(\mathbf{r}, \mathbf{r}', t')$ for any component of the fields is equivalent to the coefficients c_k^n for $t'=t-n$. These values are always the same for any time and position if the surrounding space is the same. They can be calculated beforehand and stored for posterior use.

The suitability of this approach has been established in [3]. Instead of doing the substitution for all points, the improved algorithm evaluates the surrounding cells for the position (i,j) and if there is only free space and no sources, the stored values can be used directly for c_k^n . In the other case, Gaussian substitution is done.

3. Spatial Characteristics of Radio Wave Propagation

A pulse excitation in the antenna is used here. The goal is to know how different is the propagation near the antenna and far from it, and how being in a LoS point (line of sight) is different respect to being NLoS (non line of sight). We use the next parameters for the simulation: Frequency of source = 950 MHz, cell size $\Delta s = 0.02$ m, time increment $\Delta t = 37.7$ ps, relative permittivity (concrete) = 3.0, conductivity (concrete) $\sigma = 0.005$ S/m, current amplitude = 1000 A/m^2 .

The buildings are made of concrete and they are hollow, the walls' thickness is 30 cm. The signal used is a Gaussian Pulse:

$$J_z^n = J_{\max} e^{-\alpha(t-\zeta\Delta t)^2} \quad (7)$$

Where $\alpha = -16/(100\Delta t)^2$ and $\zeta = 100$. The model is size 500m x 500m, as in fig.(1). Figure (2) shows the absolute value of E_z for the 500m x 500m model after $30000\Delta t = 1131$ ns on the sub area I of fig.(1). Figure (3) shows the absolute value of E_z for the same model after $40000\Delta t = 1508$ ns on sub area II. The propagation along the line of sight (LoS) street is direct, and the signal concentrates in a train of pulses at the wavefront, see fig(3). The propagation in diagonal direction has larger attenuation than along the vertical and horizontal directions, probably because the angle of incidence (between 30 and 60 degrees) and because there is diffraction at the corners of the buildings. If the angle of incidences is smaller, as in the left side of fig.(2), there is less reflections.

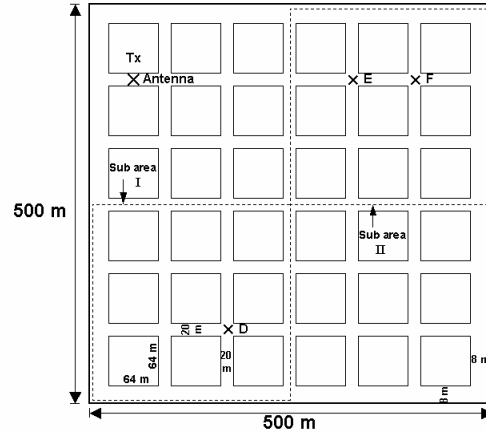


Fig.1: Urban Model of size 500m x 500m

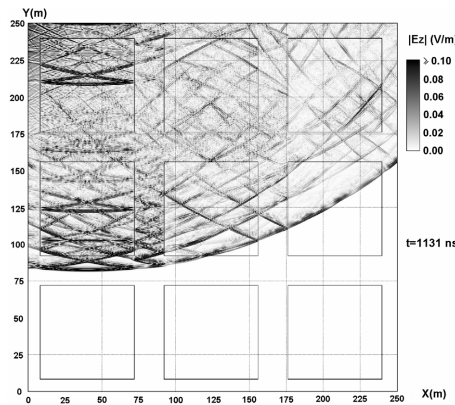


Fig.2: $|E_z|$ at sub area I (SW) at $t=1131$ ns

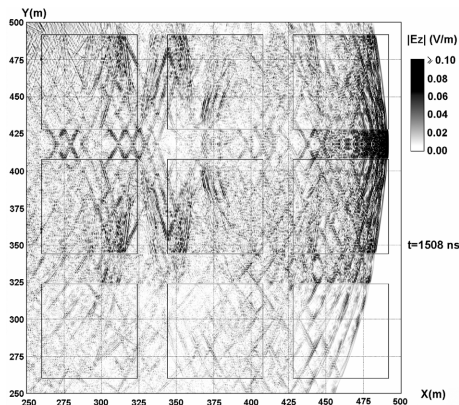


Fig.3: $|E_z|$ at sub area II (NE) at $t=1508$ ns

4. Impulse Response and Microcell Model based on FDTD results

A model using concrete hollow buildings was used, as shown in fig.(1) and parameters: cell size=0.02 m, time increment $\Delta t = 37.7$ ps, relative permittivity (concrete)= 3.0, conductivity of concrete, σ : 0.005 S/m. A Gaussian pulse modulated with carrier $f_c = 500$ MHz, $\zeta = 100$ and $\alpha = -16/(\zeta\Delta t)^2$, as shown in eq.(8), was simulated, allowing for a non negligible amount of power between 0 Hz and 1 GHz. Impulse response can be obtained by using the Fourier Transforms $F(\omega)$, $G(\omega)$ of the input $f(t)$ and output $g(t)$ respectively, in eq.(9) which gives the frequency response $H(\omega)$. Then, $H(\omega)$ is filtered by a low-pass filter with cutoff at 1.2 GHz, because the components of $F(\omega)$ are practically zero at higher frequencies. Finally, a Inverse Fourier Transform is applied to get $h(t)$. Impulse response for the Line of Sight (LoS) point F and Non Line of Sight (NLoS) point D are shown in figs.(4) and (5) respectively.

$$J_z^n = J_{\max} \cos(2\pi f_c(t - \zeta\Delta t))e^{-\alpha(t - \zeta\Delta t)^2} \quad (8)$$

$$H(\omega) = G(\omega) / F(\omega) \quad (9)$$

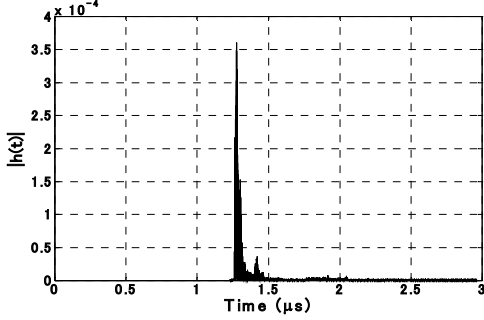


Fig.4: Impulse response $|h(t)|$ for point F (LoS)

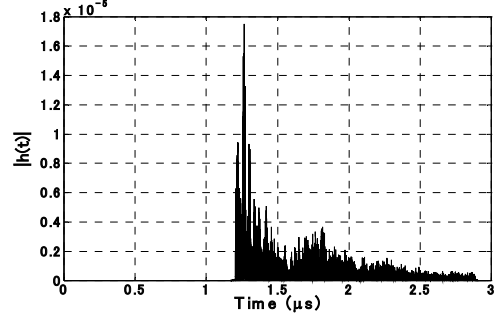


Fig.5: Impulse response $|h(t)|$ for point D (NLoS)

5. System Analysis for TDMA signals

The same model and parameters as in the previous section were used. We assumed a point antenna, generating a Gaussian pulse with a carrier $f_c = 900$ MHz and $\zeta = 6631$ as shown in eq.(8), On/Off keying. Basic signal can be considered as a set of pulses $c(t)$ for symbol 1, affected by the sequence of bits $b(t)$. For any $b(t)$, the modulated signal $d(t)$ to be transmitted can be obtained from the addition of the basic signal for all bits with value 1 adjusted with time shift, as in eq.(8). If the dynamic response of the signal in eq.(8) is E_z^* , the dynamic response for the sequence of bit represented in eq.(10) is shown in eq.(11).

$$d(t) = \sum d_i(t) = \sum J_{\max} \cos(2\pi f_c(t - \zeta\Delta t - \tau_i))e^{-\alpha(t - \zeta\Delta t - \tau_i)^2} \quad (10)$$

$$E_z(t) = \sum_{i-th \text{ bit}=1} E_z^*(t - \tau_i) \quad (11)$$

The period between signals is $T = 1 \mu s$, bit rate is 1 Mbps, and $\tau_i = (i-1)T$. For the generation of the received signal, we used the result of the FDTD simulation for only one modulated pulse (On/of keying). Then we generated the signal for a sequence of bits, using eq.(10). To recover the data, we used envelope detection, signal correlator and a detector. $BER = [P(0|1) + P(1|0)]/2$, where $P(0|1)$ is the probability of error when the original bit is 1, and $P(1|0)$ is the opposite error. Thermal noise is the source of errors; $\langle \sigma_v \rangle = 4KTBR$ is the expected variance of voltage, $K = 1.38 \times 10^{-23}$ J/°K is Boltzmann's constant, T is temperature in Kelvin ($290^\circ K = 17^\circ C$), $R = 73 \Omega$ is the resistance, $B = 80$ MHz is the bandwidth. Multipath interference affects $P(0|1)$ and $P(1|0)$. Both receptor and emitter use same antenna; power = 1 W. We generated all sequences of 6 bits ($2^6 = 64$ sequences). The total number of bits evaluated per position is 320 bits. The calculated BER is shown in fig.(6). The reception of the data is good on most of the model, except on the opposite area from the emitting antenna.

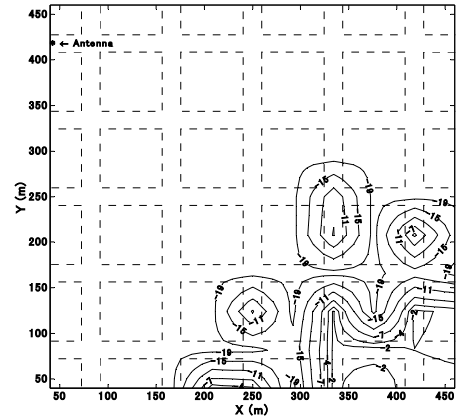


Fig.6: Calculated log(BER), 1 Mbps

6. Signal Analysis for CDMA signals

The original digital data for one channel is $b_k(t)$; it is modulated by the carrier $\cos(w_c t)$, $w_c = 2\pi f_c$ and by a high bit rate code sequence $c_k(t)$, as in eq.(12) for QPSK, and eq.(13) for D-QPSK. This signal $d_k(t)$ is transmitted and affected by multipath interference. The total transmitted signal $d(t)$ is the union of many d_k , with a different b_k and c_k . In QPSK and QAM case, the value of $\phi(c_k(t))$ is $0, \pi/2, \pi$ and $3\pi/2$ for the bits 00, 01, 10 and 11. In D-QPSK the shift is relative (cumulative), with $\psi_k(t) = \psi_k(t - T_c) + \phi(c_k(t))$, T_c is period between chips. If CDMA uses a QPSK or D-QPSK, then $\rho(c(t)) = 1$. If it uses QAM, $\rho(c(t))$ is variable. We use D-QPSK here.

$$d_k(t) = b_k(t) \cos(w_c t + \phi(c_k(t))) \rho(c_k(t)) \quad (12)$$

$$d_k(t) = b_k(t) \cos(w_c t + \psi_k(t)) \rho(c_k(t)) \quad (13)$$

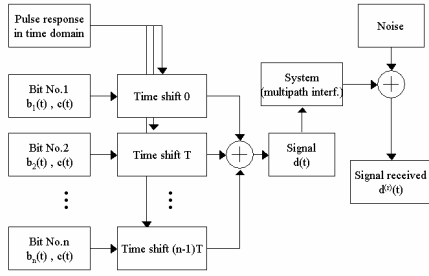


Fig.7: Diagram for generation of CDMA signal

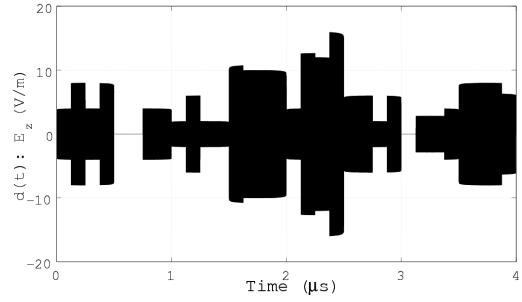


Fig.8: Total transmitted signal d(t)

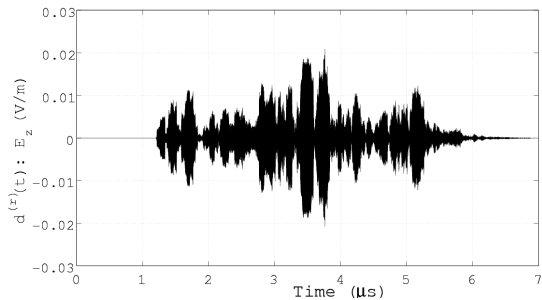
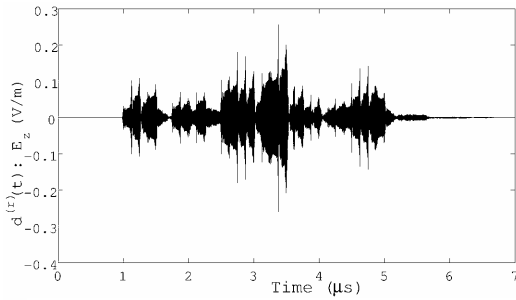


Fig.9: Total signal received $d^r(t)$, point E (LoS) Fig.10: Total signal received $d^r(t)$, point D (NLoS)

Simulation was done for 2 Mbps CDMA wireless systems, with carrier= 900 MHz, chip rate= 8 Mcps, downlink, code-set is a Gold code, 120 channels. We generate random data sequences $b_k(t)$ of 8 bits for each point, then modulated it using the $c_k(t)$ and the carrier. The summation of all channel signals $d_k(t)$ is the signal $d(t)$ to be transmitted. The signal $d(t)$ (and all $d_k(t)$) is modified by the channel into the received signal $d^r(t)$ (signal received by k-th channel is $d_k^{(r)}(t)$). The diagram for the generation of the system is shown in fig.(7). Total transmitted signal $d(t)$ is shown at fig.(8), the total received signal for point E (LoS) and D (NLoS) is shown in figs.(9) and (10) respectively. The multipath scattering deforms the signal more for point D than for point E(LoS). The original $d(t)$ has two "gaps" or time intervals without signal. In the case of point E, these gaps are visible, but for point D, only the first gap is noticeable. The original $d(t)$ has two main bursts of power. For point E, these bursts do not change much, but for point D, the second burst changes a lot.

7. Conclusions

This research began looking for a convenient algorithm for simulation of big problems using FDTD. Because of the characteristics of FDTD method, parallel processing using a new approach focused on saving memory seemed to be the best option. Parallel FDTD method is useful in the modeling of big urban channels and in the design of better systems for high-speed data communications. The merit of FDTD is better accuracy than other methods, which is important for high data rates because the broadband signals are not well simulated with other methods. This work can be used as a basis for improved system design.

References

1. Rodriguez,G. and Miyazaki,Y., "Electromagnetic Field Analysis using a Parallel FDTD Algorithm in Extremely Large Areas for Mobile Communication", Trans. IEE Japan, Vol.121-C, No.12, pp.1826 –1833, Dec.2001.
2. Rodriguez,G. and Miyazaki,Y., "Progressive Analysis of Electromagnetic Field by Parallel FDTD Algorithm for Big Urban Area 2-D Simulations", Trans. IEE Japan, Vol.122-A, No.12, pp.1031 –1037, Dec.2002.
3. Lazzi,G. and Gandhi,O., "A Mixed FDTD-Integral Equation Approach for On-site Safety Assessment in Complex Electromagnetic Environments", IEEE Trans. Ant. & Prop., Vol.48, No.12, pp.1830 –1836, Dic.2000.